7 Antenna system

7.1 Introduction

The energy for charge separation at the special pair is provided by sunlight. If sunlight is converted to electro-chemical energy, it is termed "trapping" of light energy. The absorption of a light quant and the transfer of excitation energy to the RC is performed *via* the antenna pigments. In photosynthetic organisms, the antenna pigments can be divided into three classes: Chl*a*, phycobilines and different carotenoids.

By optimising the effective antenna diameter, bacteria, algae and plants developed a huge variety of antenna systems. Beside the structural differences of diverse systems, the main goal of all systems is the optimal trapping of radiation energy over a broad wavelength range that is subsequently converted to electrochemical work. These systems have to transfer energy faster than the natural lifetime of the excited state over long distances from the peripheral antenna pigments to the ETC *via* several intermediate steps. Crucial for efficient energy transfer between pigments are the inter-pigment distances and the orientation, rather than the overall supramolecular structure of the antenna.

The most common principle of light-harvesting antenna is the "core" system found in PSII and PSI and of the reaction centre complexes of heliobacteria as well as of green sulphur bacteria. Whereas purple bacteria do not have such component, but they contain so called light-harvesting complexes (LH) 1 and 2. These two associated complexes do not show any sequence homology to the LHC of higher plants or algae. LHC I and II have circle like shape, which are built up of modules comprising two small proteins with one TMH that harbours two (LH1) or three (LH2) bacterial Chl.

The antenna system of cyanobacteria is more complex than that of purple bacteria. The "inner" antenna of PSII is formed by the two antenna proteins CP47 and CP43. In PSI the antenna is formed by the antenna domains of PsaA (40 Chl*a*) and PsaB (39 Chl*a*) as well as five low molecular weight subunits (PsaJ (3 Chl*a*), PsaK (2 Chl*a*), PsaL (3 Chl*a*), PsaM (1 Chl*a*), PsaX (1 Chl*a*). Additionally, cyanobacteria and red algae have an "outer" antenna system which is attached to the thylakoid membrane on the cytoplasmic side to increase the absorption intersection. This antenna system is consists of stacked phycobilisomes being

formed of bili proteins like allophycocyanine, phycocyanine and phycoerythrocyanine that are built up of different acyclic tetrapyrrol pigments with absorption maxima around λ = 650-550 nm. Under normal illumination these proteins are associated with PSII, but under adequate conditions they can also transfer excitation energy to PSI. The purpose of the combination of internal and external antenna systems allows optimum absorption of visible light under given conditions. In addition the flexibility in antenna size, achieved by combining the two systems in different stoichiometries, allows adaptation to different light environments.

Green algae and higher plants do not contain phycobilisomes. Instead, PSI and PSII have membrane-intrinsic LHCI and LHCII (the roman number indicates to which photosystem they belong). LHCI and LHCII are composed of trimeric homologous proteins binding Chl*a* and Chl*b*. Recently, the structure of LHCII from *Rhodopseudomonas acidophila* could be determined at 2.0 Å resolution (Papiz *et al.*, 2003). For a better understanding, the kinetics of energy transfer will be discussed below.

The energy transfer is generally described by two different theories. The Förster theory describes the radiationless energy transfer as dipole-dipole-interaction in cases of weak coupling between donor and acceptor of excitation energy. By this mechanism no electrons are exchanged between donor and acceptor. Based on this theory long distance transfer could be described, while the distance function decreases very slowly with longer distances.

The Dexter theory describes the direct overlapping of wave functions of the donor and acceptor, separated by less than 8 Å, which leads to a strong coupling. This theory could be applied for the primary electron donors of photosynthetic RC.

7.2 Antenna system of CP47 and CP43

Besides the six Chl*a* molecules in the RC of PSIIcc, the antenna subunits CP47 and CP43 bind 29 antenna Chl*a* (13 in CP47 and 16 in CP43), arranged in two layers near the cytoplasmic and lumenal sides of the membrane, an arrangement similar to that first observed in the plant LHCII (Kühlbrandt *et al.*, 1994) and PSI (Jordan *et al.*, 2001).

In contrast to PSI where the low molecular weight subunits bind 23 Chl*a*, in PSIIcc Chl*a* are only found in the antennae of CP47, CP43 as well as in D1 and D2. The cytoplasmic layers of both antenna subunits contain 9 Chl*a* molecules each (numbered Chl*a*21 to Chl*a*29 in CP47 and Chl*a*41 to Chl*a*49 in CP43), that are related by the local pseudo-*C2*(Fe^{2+}) symmetry, (Fig. 7.1). By contrast, the lumenal layer contains 7 Chl*a* in CP47 (Chl*a*11 to Chl*a*17), but only 4 in CP43 (Chl*a*33 to Chl*a*35 and Chl*a*37). The central Mg^{2+} of the Chl*a* is mostly coordinated by histidine imidazoles located in the transmembrane-spanning region (23 Chl*a*). For six Chl*a* a different coordination is observed (Table 10.4). The coordinating residues of three Chl*a* could not be determined unambiguously and they are possibly coordinated to the protein backbone, the interaction being mediated by water molecules. Indirect coordination of Chl*a* is not novel as the structures of PSI (Jordan *et al.*, 2001) and LHCII (Kühlbrandt *et al.*, 1994; Liu *et al.*, 2004) showed similar schemes. The two-layer structure of the antenna Chl*a* is in part systematic as coordinating residues located on the same TMH are often 14 residues (n and n+14) apart (Fig. 4.14and Fig. 4.16).

The overall arrangement of antenna chlorophylls is similar to the ones presented in former PSIIcc structures (Zouni *et al.*, 2001; Kamiya and Shen, 2003; Ferreira *et al.*, 2004). The orientations of some chlorin heterocycles differ between the structures, but it must be considered that their assignment might be still partially incorrect at the medium resolution level. The best indication of Chl*a* orientation in the electron density is provided by the position of its phytol chain. The current 3.2 Å resolution allowed only partial tracing of phytol chains, resulting in various reliability of Chl*a* positioning. The incompletely modelled phytol chains of Chl*a* reflect as well the higher degree of flexibility with increased distance from the conjugated chlorin ring. In our current structure we could unambiguously determine the orientation of 21 Chl*a* molecules (Table 10.4). Corresponding to 72% of the total number of Chl*a* at the current resolution and contrasts the 34 out of a total of 36 Chl*a* molecules fully modelled in Ferreira *et al.* (Ferreira *et al.*, 2004). The structure of PSI at 2.5 Å revealed 96 Chl*a* molecules of which only 47 are modelled with a full length phytol tail (Jordan *et al.*, 2001). Also in the structure of LHCII at 2.72 Å resolution, 30% of the Chl*a*/Chl*b* (Liu *et al.*, 2004) are only partially modelled. The presence of an additional Chl*a* molecule, shown in (Kamiya and Shen, 2003; Ferreira *et al.*, 2004), is not supported by our diffraction data, but can not be excluded. Consequences of this additional Chl*a* are discussed in chapter 6.4.

All Chl*a* within the antennae have neighbouring Chl*a* within the Förster radius of 16 Å. Groups of Chl*a* with centre-to-centre distance below 10.5 Å are thought to reveal strong excitonic coupling (de Weerd *et al.*, 2002b). Loosening this criteria to 12 Å (due to high expected coordinate error of 0.8 Å) we identified five such groups in CP47 (Fig. 4.12) and three in CP43 (Fig. 4.16). Their arrangement is similar between the symmetry-related Chl*a* molecules of both antenna subunits. Interestingly, Chl*a*14/34 are located deeper in the membrane interior and could assist in coupling across the membrane, thereby bridging the Chl*a* groups located in both layers.

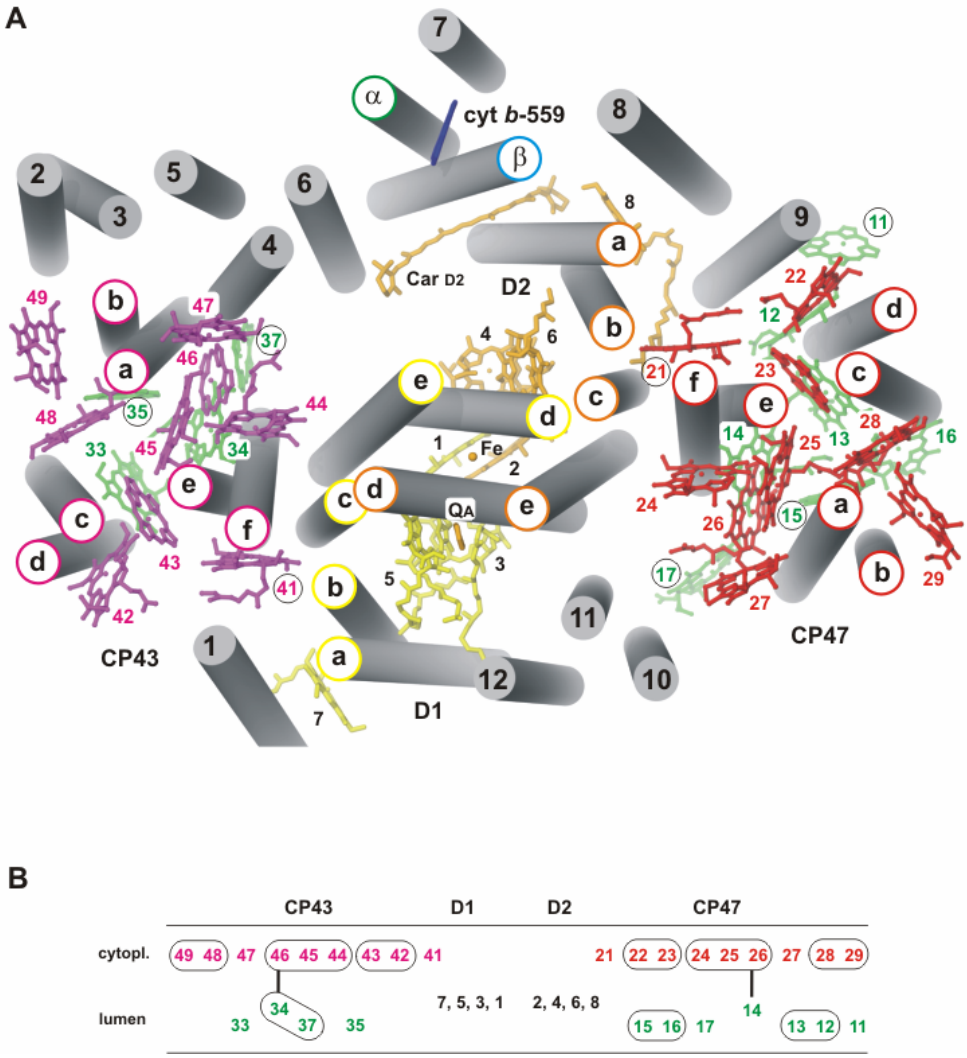

Fig. 7.1: Arrangement of cofactors in PSIIcc. (**A**) View from the cytoplasmic side on the membrane plane. Cofactors are coloured according to Fig. 4.1, except for Chl*a* in lumenal layers (green). Numbering of Chl*a* in CP43 and CP47 reflects symmetry due to the pseudo-*C2*(Fe^{2+}) rotation axis, Chl*a*(N) being related to Chl*a*(N + 20). Chl*a* with encircled numbers have no counterparts in PSI. (**B**) Arrangement of cofactors in the membrane plane. Groups of Chl*a* on layers in CP43 and CP47 closer than 10.5 Å are encircled or connected by a black line. Cofactors 1, 3, 5, 7 in D1 are equivalent to 2, 4, 6, 8 in D2.

Of special interest are Chl*a* that may connect antennae and ETC structurally and probably functionally. Chl*a*21 in CP47 is closest to $Pheo_{D2}$ in the ETC (cofactor 8 in Fig. 7.1) at a distance of 20.1 Å. The heterocycle of Chl*a*21 is well defined in the electron density and stabilised by three H-bonds donated by two adjacent serines of the protein matrix. CP47-Ser240OγH donates a bifurcated H-bond to the 13^1 and carboxymethyl carbonyl oxygen atoms (3.2 Å and 3.3 Å), and the latter also receives an H-bond (3.0 Å) from CP47-Ser239OγH (Table 10.4). The symmetry related and also well defined Chl*a*41in CP43 accepts with its 13^1 carbonyl oxygen a H-bond from CP43-Tyr274OηH and is at a distance of 21.4 Å to $Pheo_{D1}$ (cofactor 7 in Fig. 7.1). It is noteworthy that both, Chl*a*21 and Chl*a*41, do not have equivalents in PSI. A theoretical study suggested that Chl*a*21, Chl*a*41 contribute about 50% and Chl*a*24, Chl*a*44 about 25% to the total transferred excitation energy between antennae and the ETC (Vasil'ev *et al.*, 2003; Vasil'ev and Bruce, 2004). It seems that Chl*a*21 and Chl*a*41 play a role in energy transfer to the ETC rather than $Chlz_{D1}$ and $Chlz_{D2}$ (cofactors 7 and 8 in Fig. 7.1), in agreement with a spectroscopic study suggesting that the energy transfer involving the two Chlz is likely to be slow (Schelvis *et al.*, 1994). In PSI two Chl*a* (aC-A40 and aC-B39) seem to connect the antenna system with the ETC. In PSI the distance of these two Chl*a* (12.8 and 10.9 Å) to the ETC is much closer than that of Chl*a*21 and Chl*a*41 to the ETC in PSII. The question arises whether there is another cofactor involved in excitation energy transfer in PSIIcc? The gap between the antenna system and the ETC could be functionally bridged by Car that could not be yet be located. It should also be noted that Chl*a*21 and Chl*a*41 are located at the interface of D2 and CP47 as well as D1 and CP43 (Fig. 7.1). This interface differs from that of PSI, where the antenna and RC domain belong to one single protein (PsaA and PsaB).

After Chl*a*21, Chl*a*24 is the second closest (24.6 Å) to the cofactors of the ETC. Mutational studies combined with spectroscopic investigations suggested Chl*a*24 (Eaton-Rye and Vermaas, 1992), as well as Chl*a*25 and Chl*a*29 to be important for the function, and the latter two also appear to be essential for the stable assembly of PSIIcc (Shen and Vermaas, 1994). Fluorescence emission spectra on CP47-His114 mutants suggested that Chl*a*29 could be associated with the 695 nm emission peak originating from a very small number of Chl*a* molecules (van Dorssen *et al.*, 1987; Shen and Vermaas, 1994; de Weerd *et al.*, 2002a). CP43 is not known to harbour a Chl*a* molecule with such spectroscopic characteristics, and mutation studies of the equivalent residue did not show any change in the spectrum (Manna and Vermaas, 1997).

Stark spectroscopy indicated about three Chl*a* that are part of the excitonically coupled system in CP47, absorb at 683 nm and are arranged close together (de Weerd *et al.*, 2002a). In CP47 the five Chl*a* (Chl*a*14/Chl*a*17 and Chl*a*24 to Chl*a*26) form a group that would satisfy these geometrical conditions (Fig. 7.1). This situation is mirrored in CP43, since here five Chl*a* are strongly coupled (Chl*a*34/Chl*a*37 and Chl*a*44 to Chl*a*46). Interestingly, Chl*a*44, which is better defined in the electron density compared to the others, is the second closest (24.3 Å) to the cofactors $Pheo_{D1}$ of the ETC (cofactor 5 in Fig. 7.1) and stabilised by π-stacking with CP43-Trp443. According to a theoretical study, Chl*a*44 contributes notably to the energy transfer to $Pheo_{D1}$ (Vasil'ev *et al.*, 2003). Stark measurements suggest that at least three to five Chl*a* molecules could contribute to this excitionically coupled system (Groot *et al.*, 1999), which is in good agreement with our findings. Mutations of CP43-His53 coordinating Chl*a*45, one of the central Chl*a* within its group, showed a significant change in fluorescence decay kinetics (Manna and Vermaas, 1997). Note that similar effects were observed for Chl*a*25, its counterpart in CP47.

The second frequent by occurring cofactor within the antenna system is Car. Spectroscopic analysis predicted the presence of 9 ± 1 *β*-carotene molecules per PSIIcc monomer in our crystals (Kern *et al.*, 2004a). The electron density at 3.2 Å contains several elongated patches which might correspond to β-carotene, lipid or phytol chain fragments. As a clear assignment of such density is unreliable at this resolution, we decided to model in "dummy atom" aliphatic chains to indicate positions of possible cofactor fragments.

In contrast, Ferreira *et al*. (Ferreira *et al.*, 2004) modelled 6 additional *β*-carotene molecules within one PSIIcc monomer, 4 at the interface between CP43 and various small subunits and two at the side of CP47. From our 3.2 Å electron density we can not confirm the positions of these Car. Only for one of them (at the side of CP43) we have found a patch of elongated electron density in a partly similar position which could be occupied by a carotenoid. At the present resolution no statement can be made about the nature of the carotenoids and it can not be excluded from the structural data that also other forms of carotenoids apart from β-carotene are present in PSIIcc.